# Shape, Size, and Distribution of Ca$^{2+}$ Release Units and Couplons in Skeletal and Cardiac Muscles

Clara Franzini-Armstrong,* Feliciano Protasi,* and Venkat Ramesh[#]

*Department of Cell and Developmental Biology, School of Medicine, University of Pennsylvania, Philadelphia, Pennsylvania 19104; and
[#]Department of Cardiology, Children's Hospital of Philadelphia, Philadelphia, Pennsylvania 19104 USA

ABSTRACT   Excitation contraction (e-c) coupling in skeletal and cardiac muscles involves an interaction between special-ized junctional domains of the sarcoplasmic reticulum (SR) and of exterior membranes (either surface membrane or transverse (T) tubules). This interaction occurs at special structures named calcium release units (CRUs). CRUs contain two proteins essential to e-c coupling: dihydropyridine receptors (DHPRs), L-type Ca$^{2+}$ channels of exterior membranes; and ryanodine receptors (RyRs), the Ca$^{2+}$ release channels of the SR. Special CRUs in cardiac muscle are constituted by SR domains bearing RyRs that are not associated with exterior membranes (the corbular and extended junctional SR or EjSR). Functional groupings of RyRs and DHPRs within calcium release units have been named couplons, and the term is also loosely applied to the EjSR of cardiac muscle. Knowledge of the structure, geometry, and disposition of couplons is essential to understand the mechanism of Ca$^{2+}$ release during muscle activation. This paper presents a compilation of quantitative data on couplons in a variety of skeletal and cardiac muscles, which is useful in modeling calcium release events, both macroscopic and microscopic ("sparks").

## INTRODUCTION

Rapid release of Ca$^{2+}$ from the sarcoplasmic reticulum (SR) is a key event in excitation contraction (e-c) coupling of both skeletal and cardiac muscles. SR Ca$^{2+}$ release is pre-dominantly under the control of the exterior membranes—surface membrane and transverse (T) tubules—whose de-polarization initiates e-c coupling events. Functional interaction between external membranes and SR involves two Ca$^{2+}$ permeant channels: the dihydropyridine receptors (DHPRs, or L-type Ca$^{2+}$ channels) of exterior membranes, and the ryanodine receptors (RyRs) or SR calcium release channels. The latter are visible as "feet" in electron micro-graphs from thin section.

Discrete junctional domains of the SR (jSR), containing RyRs, interact with specialized junctional domains of sur-face membranes and/or T tubules, containing DHPRs. The interaction occurs at intracellular junctions, named dyads, triads, and peripheral couplings. Dyad is the apposition of a junctional SR cisterna (jSR) to a short T tubule segment; triad is the apposition of two jSR cisternae on either side of a T tubule segment; peripheral coupling is the apposition of a jSR cisterna to an approximately circular junctional do-main of the surface membrane. In cardiac muscle special jSR domains bearing RyRs, but not associated with the surface membrane, are also present (corbular or extended junctional SR, EjSR, Jewett et al., 1973; Anderson et al.,

1976; Junker et al., 1994; Sommer, 1982, 1995; Sommer et al., 1991; Carl et al., 1995). All the above junctions are functionally equivalent and they are collectively called cal-cium release units (CRUs). The junctional domains of SR and exterior membranes constituting CRUs are separated from each other by nonjunctional domains of the two mem-branes, which contain a different complement of proteins (Franzini-Armstrong and Jorgensen, 1994; Franzini-Arm-strong, 1996).

A further, useful dissection of the system involves the concept of "couplon" (Stern et al., 1997; Rios and Stern, 1997). A couplon is the functional grouping of RyRs and DHPRs (and other junctional SR proteins) which may act in concert during e-c coupling. According to this definition, a triad contains two couplons, one on either side of the T tubule, which act independently of each other. Dyads and peripheral couplings are constituted of a single couplon each (Sommer et al., 1998).

Modeling of the interactions between DHPRs and RyRs within a couplon and of the interactions between adjacent calcium release units requires specific knowledge of the constraints imposed by geometrical and topological factors. Two geometrical factors are constant in all types of CRUs. One is the size of the junctional gap separating SR from exterior membranes (10–12 nm) which is apparently deter-mined by the size of the RyR's cytoplasmic domain or foot; the other is the tight, ordered clustering of feet. In skeletal muscle feet are arranged in a tetragonal disposition with an approximate center-to-center distance of 29 nm. In cardiac muscle the feet are disposed at regular intervals approxi-mately equal to those in skeletal muscle (Sommer et al., 1998), but the precise parameters of their disposition are not known. Three geometrical factors, the shape and size of the units, and the distance separating them from each other are widely variable between different types of fibers. Despite

the abundant morphometric data available in the literature, very little information is available on these variable factors. This work provides a compilation of data that may be useful in modeling events within the CRUs as well as possible interactions between them. The data are collected from a large variety of muscles.

## METHODS

### Thin sectioning

Hearts from adult chicken, mouse, rat, and dog and skeletal muscles from toadfish, frog, rat, and guinea pig were fixed either by perfusion (all hearts and some skeletal muscle) or by immersion in fixative. Perfusion was with a Ca$^{2+}$-free solution (0.9% saline with or without 10 mM potassium phosphate buffer, 10 mM EGTA pH 7.4) followed by 3.5–6% glutaraldehyde in 0.1 M cacodylate buffer pH of 7.4. Heart muscle was perfused either through the left ventricle or aorta; leg muscles through the descending aorta and toadfish swimbladder through a local artery. Perfused muscles were stored in the fixative. Small pieces of muscle were post-fixed in 2% osmium tetraoxide in 0.1 M cacodylate buffer for 2 h, en-bloc stained in saturated uranyl acetate at 60°C for 4 h, and embedded in Epon 812. Thin sections were stained with uranyl acetate and a combination of lead salts and viewed in a Philips 410 electron microscope.

### Golgi staining

Skeletal muscles fixed in glutaraldehyde were sequentially infiltrated with potassium dichromate-osmium tetraoxide and with silver nitrate, as described in Franzini-Armstrong and Peachey (1982), Franzini-Armstrong et al. (1987, 1988), and Appelt et al. (1989, 1991). Semithin sections (~¼ $\mu$m thick) were observed at 100 KV accelerating voltage.

### Freeze-fracture

Skeletal and cardiac muscles were fixed in 3.5–6% glutaraldehyde as above, infiltrated in 30% glycerol, frozen in liquid nitrogen-cooled propane, fractured, shadowed with platinum at 45°, and replicated with carbon in a Balzer 400.

### Measurements

Measurements were taken on sets of micrographs that were either collected for this purpose or part of the laboratory archives, having been collected for past studies. Criteria of micrograph selection and sample size varied somewhat and this is detailed below for individual cases.

Specific methods of measurement are given in the Results section. Note that the micrographs were taken over a prolonged period of time, but with two exceptions, they were collected using two calibrated microscopes in which variations in magnification are estimated to be at most 5%. The one exception is the slow tonic muscle in the frog, in which an error of up to 10% may exist in the data.

### Comments on data reliability

Three factors affect the reliability and applicability of quantitative EM data. One is the data collection, the second is the sample size, and the third is the selection criteria (if not random). These factors vary somewhat for the various muscles used in this work and are detailed below.

#### Criteria for data collection

The data were collected in two stages: an initial set of micrographs was obtained and a subset of these micrographs was used for the measurements.

*Initial data collection.* The data for the first 10 muscles in Table 1 (toadfish very fast to toadfish very slow) were obtained from Golgi-stained sections. The initial sets of micrographs for these muscles were obtained under standard criteria of randomization, as follows. The Golgi infiltration is randomly successful within a bundle of muscle fibers: some fibers have infiltrated T tubules while others do not, and the effect is totally independent of any obvious factor (such as fiber type, etc.). By photographing either all infiltrated fibers or all the fibers of a certain type in a given cross-section, we obtained a random sample of the fibers in each muscle, which was usually very large. In the case of toadfish, rat, and guinea pig, this sample was originally used for quantitation of feet content (see Franzini-Armstrong et al., 1988; Appelt et al., 1989, 1991). The data for the slow tonic fibers of the toadfish come from a single fiber.

For CRU size in the frog slow tonic fibers thin sections were used. Images were collected from all areas of the sections that showed CRUs. The sample size was naturally limited by the fact that few tonic fibers are present in the muscle.

For CRU size and inter-CRU distance in chicken and mouse cardiac muscle (Table 2) micrographs were taken only in areas where the orientation of the fibers was as good as possible. For the chicken, all fibers with a good transverse orientation were photographed; for the mouse muscle, pictures were systematically taken along a well-oriented bundle of fibers. Stringent randomization criteria were not used in collecting the photographs from dog and rat myocardium. In these muscles images were taken in areas of the section that showed well-oriented CRUs. Smaller CRU

## TABLE 1  Size of couplons in skeletal muscle

| Source | Muscle type (No. T segments measured) | No. of feet per couplon Average (range) |
|---|---|---|
| Toadfish, female | Very fast twitch (swimbladder) ($n = 30$) | 56 (13–115) |
| Toadfish, male | Very fast twitch (swimbladder) ($n = 30$) | 18 (9–24) |
| Rat | Fast twitch (EDL) ($n = 30$) | 38 (16–71) |
| Guinea pig | Fast twitch (wh. vastus lat.) ($n = 30$) | 34 (9–64) |
| Frog | Twitch (ileofibularis) ($n = 30$) | 36 (13–63) |
| Frog | Twitch (semitendinosus) ($n = 30$) | 29 (14–60) |
| Rat | Slow twitch (soleus) ($n = 30$) | 24 (9–45) |
| Guinea pig | Med. twitch (red vastus lat.) ($n = 30$) | 24 (13–39) |
| Guinea pig | Slow twitch (soleus) ($n = 30$) | 17 (7–27) |
| Toadfish | Slow tonic (swimbladder) ($n = 30$) | 30 (15–135) |
| Frog | Slow tonic (cruralis) ($n = 30$) | 35 (NA*) |

A couplon, as defined by E. Rios, is a group of RyRs immediately adjacent to each other and thus interacting with each other during e-c coupling. Triads have two couplons, dyads and peripheral couplings have one couplon each.

*The number was obtained by calculating an average diameter from individual chord measurements (see text), and thus range is not available.

**TABLE 2  Size of couplons in cardiac muscle**

| Source | CRU type | No. of feet per couplon |
|---|---|---|
| Chicken left ventricle | Peripheral couplings ($n = 30$) | 29–32 |
| | Extended jSR ($n = 30$) | 37* |
| Dog left ventricle | Peripheral couplings ($n = 63$) | 61* |
| | Dyads ($n = 28$) | 90* |
| Rat left ventricle | Dyads ($n = 30$) | 267* |
| Mouse left ventricle | Peripheral couplings ($n = 30$) | 150* |
| | Dyads ($n = 30$) | 128* |

*This number assumes that the junctional patches of membrane are approximately round.

profiles were included in the micrographs, but some may have been missed.

Measurements of CRU interdistances (Table 3) in toadfish and frog skeletal and in chicken cardiac muscles were obtained either from randomly collected images of sectioned cells (as described above), or from freeze-fracture (FF). Random FF images were collected by taking one low power photograph covering a long segment of each of the fibers whose plasma membrane was visible in the fractures. Interdistances in mouse and rat myocardium were obtained from serial section reconstructions in cross-sections of two and one fiber, respectively. Fiber selection was "random" in the sense that the only criteria dictating it were orientation of the fiber in the section and the ability to follow the fibers through many sections without wrinkles and other section defects.

*Selection of micrographs for measurements.* A small number of micrographs (three from three different fibers) was used for measuring CRU sizes of skeletal muscles 1–9 in Table 1. Criteria for their selection from the initial set of data are as follows. In the case of toadfish swimbladder and of frog muscles the fibers are basically identical to each other, and the selection was random: we opened the book of micrographs and selected the first three that showed good preservation and section orientation. In the case of rat and guinea pig muscles we selected the first three fibers which, in addition to being well-preserved and appropriately cut, were also typical of the fiber type as defined in our previous quantitative studies (Franzini-Armstrong et al., 1988; Appelt et al., 1989). For guinea pig muscle, for example, the fibers selected had ~90, 80, and 35% of their T tubules covered by junctional SR (see Fig. 14 in Franzini-Armstrong et al., 1988). In all cases size measurements were started in the center of the image and all CRUs along the T tubule network were measured until the appropriate sample size was obtained. The toadfish tonic fiber was single-fiber and thus it represents an "example"; all micrographs from the tonic frog fibers were used for measurements. For measurements of CRU size, either the first 30 CRU profiles, or (in the case of dog heart) all the profiles seen in the available set of micrographs, were measured.

For inter-CRU distances in toadfish and frog skeletal muscle micrographs used were a large sample and were randomly selected as above. For chicken cardiac muscle all inter-CRU distances from all available micrographs of well-oriented cross-sectioned fibers and of FF fibers were measured. For rat and mouse cardiac muscles distances were obtained from 3-D reconstructions of one and two fibers, respectively.

With one exception, the data for skeletal muscle were obtained from "Golgi-stained" samples. This technique gives micrographs that are ideal for measuring the size of CRUs, because the entire CRU and nonjunctional T tubule segment are visible in the image and a direct measurement is possible. A sample size of 30 units is quite representative of the population.

In the case of frog slow fibers and cardiac muscle, couplon sizes were determined from thin sectioning. In this case, the size of the profile is determined both by the size of the CRU and by the positioning of the section relative to the CRU. The data obtained in this manner are less precise and should be taken as "estimates" rather than absolute values when the sample size is 30 or less.

Values for inter-CRU distances in toadfish and frog skeletal and in chicken cardiac muscle are obtained from a large sample and thus applicable to the whole muscle; those from rat and mouse cardiac should be taken as "samples" because they represent only one and two fibers, respectively.

*Sample selection*

In the case of rat and guinea pig skeletal muscles, the micrographs used in the measurements were specifically selected to be representative of the major fiber and do not represent an average of all fibers within a given muscle. In all other cases, criteria for selecting micrographs were based exclusively on criteria such as quality of fixation, presence of sufficient number of CRUs in the image, and appropriate orientation of the section. None of these criteria affect "random" sampling.

## RESULTS

Four sets of data are given: the shape of CRUs, the size of couplons (given as feet content), the disposition of couplons (given as number of feet that may be present in a small volume of fiber), and the minimum distances between neighboring CRUs.

## The shape of CRUs and the disposition of feet in skeletal and cardiac muscle

The shape and size of the membrane domains from SR and T tubule that participate in the formation of CRUs affect the properties of the restricted volume within the junctional gap separating the two membrane systems. The larger and more rounded the membrane domains, the more likely that calcium release results in a temporary trapping of calcium in the junctional gap, that is, in a brief rise in calcium concentration to values higher than in the surrounding cytoplasm. In twitch skeletal muscles, CRUs are in the form of triads (Fig. 1 *A*), which have an elongated shape in the transverse
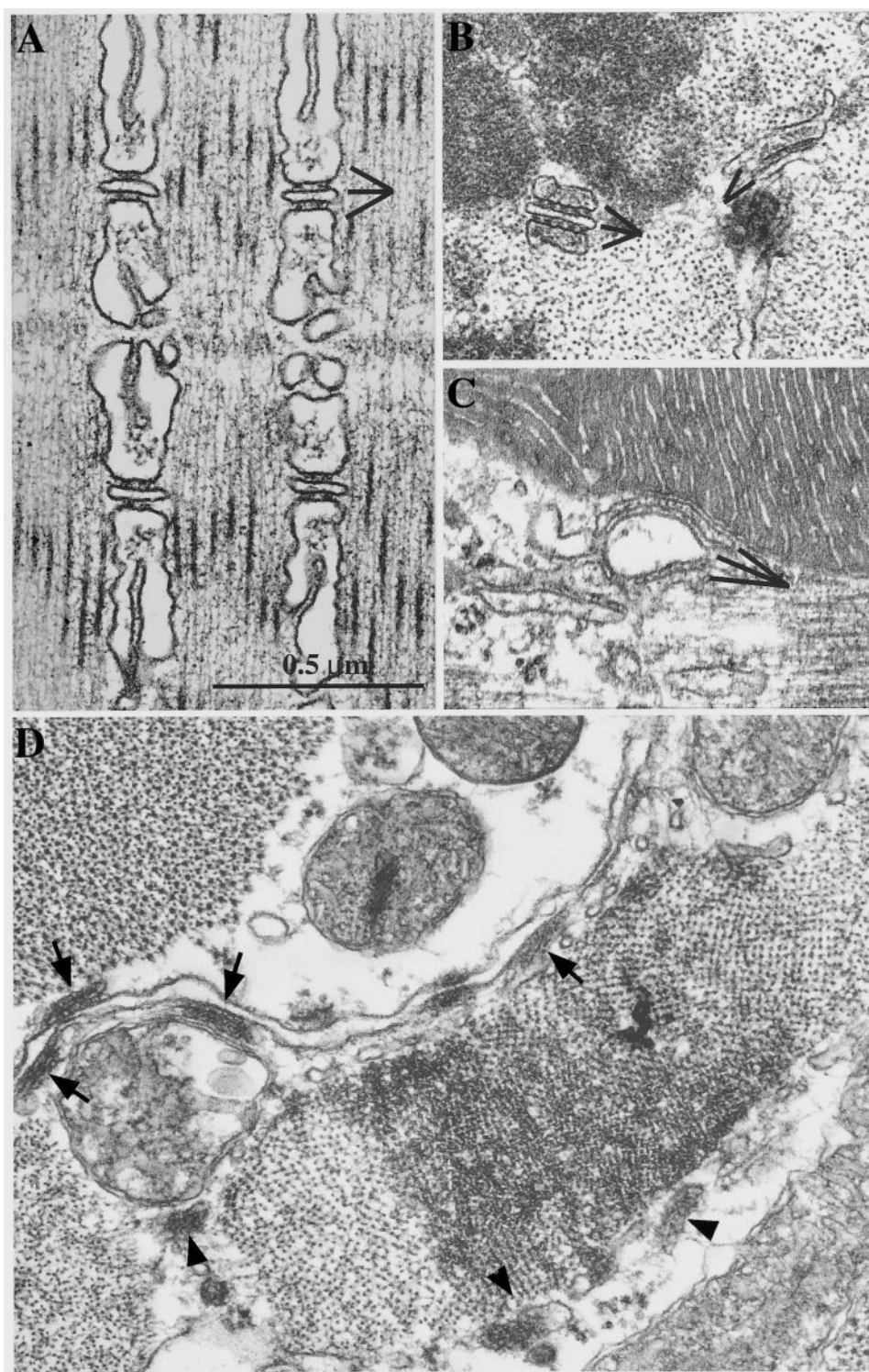
**TABLE 3  Minimum distances between CRUs in cardiac and skeletal muscle**

| Source | Muscle type | Peripheral couplings | Internal units |
|---|---|---|---|
| Toadfish skeletal | Very fast twitch | | 107 ± 2 nm (359)* |
| Frog skeletal | Twitch | | 103 ± 2 nm (238)* |
| Toadfish skeletal | Slow tonic | | 700 ± 35 nm (60)* |
| Chicken cardiac | Left ventricle | 472 ± 5 nm (340) | 148 ± 6 nm (287)* |
| Rat cardiac | Left ventricle | | 414 ± 24 nm (25)* |
| Mouse cardiac | Left ventricle | | 313 ± 21 nm (73)* |

*Mean ± SEM (No. of measurements).

FIGURE 1   Junctions between the sarcoplasmic reticulum and exterior membranes have varying geometries. (*A*) Toadfish swimbladder muscle. Triads (three lines) are junctions between one segment of the T tubule network and two apposed SR elements. The transverse tubules are flat ribbons with two narrow surfaces facing wide SR cisternae. The junctional surfaces are oriented transversely to the direction of the filaments. (*B*) Triad (three lines) and dyad (two lines) in a tonic fiber from the frog. The junctional T tubule segments have the shape of flat disks and either one or two flat SR cisternae are apposed to them. The junctional surfaces are oriented longitudinally, or parallel to the direction of the filaments. (*C*) An internal junction between SR and a T tubule in mouse left ventricle. Two SR elements are apposed to a wide dilated T tubule profile. The junctional surfaces are oriented longitudinally. Note that the two SR elements are probably continuous with each other in a plane just above or below the image. (*D*) Peripheral couplings (*arrows*) are junctions between one SR vesicle and the surface membrane, as seen in a cell from the chicken left ventricle. Other SR elements in the fiber interior (*arrowheads*) have junctional components (feet and calsequestrin) but are not associated with exterior membranes. These are called corbular and/or extended junctional SR.

plane (Fig. 2, *A* and *B*). The junctional gap is occupied by two rows of feet and all feet are in equivalent position, with one side facing the junctional gap and one facing the myofibrils (see Franzini-Armstrong and Jorgensen, 1994, for a review). While wider jT segments bearing three rather than two parallel rows of feet has been reported (Appelt et al., 1991), in our experience this configuration is rare in twitch fibers of vertebrates. This geometry has been taken into consideration in recent modeling (Rios and Stern, 1997; Stern et al., 1997; Pape et al., 1998), with different conclusions. In CRUs of frog slow-tonic fibers dyads and triads are composed of junctional domains of SR and exterior membranes with ovoid or circular shapes (see Figs. 1 *B* and 2 *C*) and thus contain short, but multiple rows of feet (Page, 1965; Franzini-Armstrong, 1973). In cardiac muscle, dyads, triads (Fig. 1 *C*), and peripheral couplings (Fig. 1 *D, arrows*) involve round or ovoid patches of membrane, which

also contain multiple rows of feet (Page and Niedergerke, 1972; Sommer, 1982, 1995). Some of these junctions are quite large. In junctions with a circular profile of the junctional membrane domains, feet at the edges of the junction are not in identical conditions relative to feet in the middle of the junctions. The latter are at a longer distance from the edge of the junctional gap, and are thus contained within a space with possible calcium trapping properties. In the case of corbular SR and EjSR (Fig. 1 *D, arrowheads*), all feet are fully exposed to the cytoplasm and no trapping space exists (Dolber and Sommer, 1994; Sommer et al., 1997).

In vertebrate skeletal muscle feet are not detected in areas of the SR that are not directly facing T tubules. However, immunolabel experiments (Dulhunty et al., 1992) have indicated the possibility that extrajunctional ryanodine receptors are located in the membrane of the terminal cisternae, in proximity of the T tubules, but not facing them. Presum-
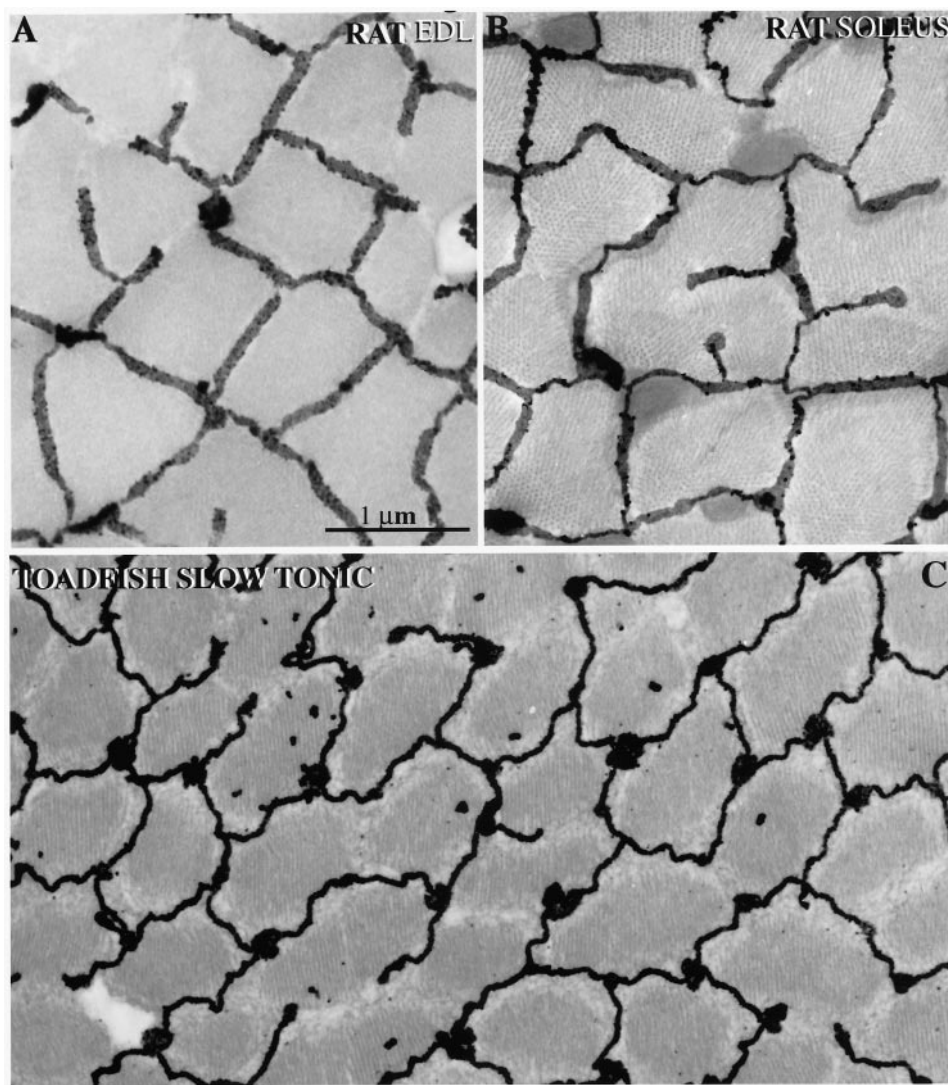


FIGURE 2   Cross-sections through Golgi-infiltrated muscle fibers from the rat EDL (*A*) and soleus (*B*) and from a presumed tonic fiber in the toadfish swimbladder (*C*). The EDL soleus fibers are representative of fast-twitch and slow-twitch fibers, respectively. The lumen of T tubules is filled by an electron-dense precipitate that outlines the shape of the tubules. The wider ribbonlike segments in the twitch fibers and the rounded disks in the slow fiber are junctional segments of the T network. A decreasing portion of the T network forms junctions with the SR as one progresses from *A* to *C*.

ably the cytoplasmic domains of these extrajunctional RyRs are not detected by electron microscopy because they are not clustered. Alternatively, the RyRs that are detected by these antibodies have a truncated cytoplasmic domain. Indeed, rows of intramembrane structures resembling RyRs, but not rows of feet, have been in the perijunctional region of the frog skeletal muscle SR by FF (Franzini-Armstrong, unpublished observations). Clusters of feet in areas of SR not associated with T tubules are quite visible in cardiac muscle, where they constitute the extended junctional or corbular SR (see Introduction).

## The size of couplons, skeletal muscle

Measurements were taken on cross-sections of Golgi-infiltrated muscles in which the outlines of the T tubules are very clearly delineated (Fig. 2, *A–C*). T tubule networks contain two types of tubule segments: wide segments with a flattened cross-section (jT) that are junctional, and thinner segments with a wavy path (free T), that simply join the junctional segments to each other.

### Twitch fibers

The jT segments constitute the central elements of triads and thus participate in two couplons, one on either side. Dyads are rare, but slightly more frequent in slow-twitch than in fast-twitch fibers (Dulhunty, 1984). In the great majority of jT segments the flat surfaces are just wide enough to be occupied by two rows of feet running parallel to the T tubule axis. The rare segments that accommodate three rows are ignored in the calculations. Feet are evenly spaced along the two rows and interruptions in the spacing are not observed within a jT segment. The length of jT segments was directly measured on the micrographs, and the number of feet belonging to the couplon covering one side of the jT segment was obtained by dividing the length of the segment by 29 nm (the average distance between feet in both skeletal and cardiac muscle; Cullen et al., 1984; Block et al., 1988; Dulhunty, 1989; Sommer et al., 1998) and multiplying by 2. The results are given in Table 1. The muscle type and the number of T segments measured are given in column 1; the average, minimum, and maximum couplon sizes are given in column 2.

### Tonic fibers

Tonic fibers were identified in the frog and sand dab by correlating ultrastructural and functional features (Peachey and Huxley, 1962; Page, 1965; Franzini-Armstrong et al., 1987). Identification of the rare tonic type fibers in the toadfish swimbladder was solely based on similarity of myofibril size and membrane system disposition with those of the well-identified tonic fibers. The junctional T tubule segments in tonic fibers are short and have an approximately round profile; the nonjunctional segments are very

long. CRUs are composed of apposed flat round T tubule segments and flat SR cisternae of similar shape and they may be either dyads or triads (Figs. 1 *B* and 2 *C*). The junctional gap is occupied by multiple rows of feet in a tetragonal arrangement. The area of the junction was either measured directly in Golgi-infiltrated fibers (for the toad-fish, Fig. 2 *C*), or calculated from measurements of random chords through the approximately circular junctions, as seen in thin sections (for the frog tonic fibers, Fig. 1 *B*). In this latter case, the diameter (*D*) of the junctional patch is related to the average chord (*Y*), as follows: $D = y\pi/4$. The number of feet/couplon was determined by dividing the area of the flat pancake by 29 $nm^2$.

All couplons in skeletal muscle fibers are composed of a fairly large number of feet, the minimum being about 10, the maximum up to and above 100. As indicated by the range, the variability is fairly large even within a single fiber type. The data in Table 1 are arranged in order of decreasing muscle speed, from the superfast muscle fibers of the toad-fish swimbladder, which have a very rapid calcium transient and operational frequency of up to 200Hz (Rome et al., 1996), to the fast-twitch and slow-twitch type fibers of mammals and amphibia, with contraction-relaxation cycles in the 40–100 ms range, to the tonic fibers which are 10 times slower and are capable of a prolonged contracture (Costantin et al., 1967; Gilly and Hui, 1980; Gilly and Aladjem, 1987). One noticeable trend in the table is the decreasing size of the couplon in parallel with the increasing contraction time. This is due to the fact that in slower fibers the junctional T tubule segments are shorter and the non-junctional segments proportionally longer (Fig. 2), resulting in an overall lower density of feet per fiber volume. The muscles of lizards, animals well known for their rapid movements, also have very long stretches of junctional SR (Forbes and Sperelakis, 1980). Two noticeable exceptions to this relationship between fiber speed and size of couplons exist. One exception is the muscle from the male toadfish, which is as fast as that of the female, but has much shorter junctional T tubule segments and thus couplons containing fewer feet. The overall density of feet per fiber volume in the male swimbladder muscle is as high as that in the female due to the very short length of the free segments connecting the junctional ones. At the other end of the range, the couplons in tonic fibers contain as many feet as those in fast or super-fast twitch fibers, due to the oval shape of the junctional surfaces, which accommodate several rows of feet. However, the overall density of feet per fiber volume in the slow fibers is low, due to a large distance separating junctional segments from each other.

## The size of couplons, cardiac muscle

The size of couplons was determined by measuring the length of the junctional SR profiles in images from thin sections (see Fig. 1 *D*). The profiles are random chords cut through the junctional surface. The content of feet in an

average couplon was estimated by assuming that the shape of the junctional SR surface is circular and using the previously established relationship between a random chord, the diameter of the circle, and the feet content (see tonic fibers above) and the results are shown in Table 2. The accuracy of this estimate varies for the three types of CRUs present in cardiac muscle: peripheral couplings, dyads (triads), and extended junctional SR. In the case of peripheral couplings, the shape is quite close to circular and the estimated area is a good approximation of the actual area (see Protasi et al., 1996). Dyads tend to have a profile that is elliptical, with the long axis of the ellipse transverse to the fiber long axis (see Forbes et al., 1984, 1985; Forbes and van Niel, 1988; Forbes, 1990). The average diameter may be skewed either toward too short or too high a value if the sections happen to be predominantly parallel to either the long or the short axis of the ellipse. Since measurements were taken in longitudinal sections, shorter profiles cutting directly across the junction dominate over longer profiles that follow the length of the junction, resulting in an underestimated area. Extended junctional SR is also elongated in a transverse direction. Measurements for this component of the chick myocardium were taken from transverse sections, and thus the calculated surface is likely to be overestimated.

Couplons in chicken cardiac muscle are quite comparable in size to those in skeletal muscle. However, couplons in mammalian cardiac muscle tend to be quite large and have a content of feet that is as large as, or considerably larger than, that of the fastest skeletal muscle, despite the fact that myocardium does not reach as high a frequency of contraction. As for skeletal muscle, there is a general tendency for couplons to be larger in myocardium, with a faster functional frequency, that is in smaller animals, although the rat may prove to be an exception.

## The disposition of CRUs

In both skeletal and cardiac muscle, CRUs are located mostly along the T tubule networks. The networks are located either in a single transverse fairly narrow band at the level of the Z line, or in two bands close to the Z line and symmetrically located relative to it. In adult skeletal muscle, longitudinal extensions of the T tubule network do not form junctions with the SR. In cardiac muscles, longitudinal extensions are more frequent and do form occasional junctions with the SR at variable distances from the Z line. Four factors affect the disposition and frequency of CRUs within the transverse bands containing T tubule networks. One is the size and shape of the myofibrils, which determine the position of the T tubules within each transverse tubule network; a second is whether one or two T tubule networks are located either in correspondence of the Z line or on both sides of it; a third factor is the distance between CRUs, which is in turn determined by the length of nonjunctional T tubule and/or by the area of surface membrane intervening between neighbors CRUs; a fourth factor is the combi-

nation of size and shape of the CRUs. The following analysis of CRU dispositions is aimed at providing information relevant to the detection of small calcium release events (sparks), which are generated at CRU sites.

### Skeletal muscle

Ideally, a line scan image of the type used in detecting sparks samples an $\sim 1$-$\mu$m-thick slice and may have a resolution of $\frac{1}{2}$ $\mu$m in the $x/y$ plane. In order to provide data relevant to the confocal images, the disposition of CRUs was analyzed as follows. 1) The contrast of a micrograph from a cross-section of a Golgi-stained muscle fiber (such as shown in Fig. 2, but larger in size) was enhanced so that only the T tubule network is visible. 2) The nonjunctional segments of the T network were erased, leaving only the wide junctional segments belonging to CRUs in the image; 3) several 1 $\mu$m by 15–17 $\mu$m strips were cut from the cross-sectional image, and presented separately; 4) a "selection window" $\frac{1}{2}$ $\mu$m in width and 1 $\mu$m in depth was moved at $\frac{1}{4}$ $\mu$m intervals from left to right along the strips; 5) the total length (in nm) of junctional T tubule segments within the window was measured at each position and multiplied by $\frac{4}{29}$ to obtain the number of feet.

Figs. 3–6 show the results for four representative types of muscle fibers: a fast-twitch fiber from rat EDL, a slow-twitch fiber from rat soleus, two fibers from the frog ileofibularis, and a tonic fiber from toadfish swimbladder, all illustrated at the same magnification of 21,300. In each figure, a strip showing the real image is shown immediately above a histogram showing the number of feet contained within each selection window along the strip. Four bars of the histogram and the height of the strip represent distances of 1 $\mu$m. Glancing across the strips in the top-to-bottom direction gives a good idea of what parts of a T tubule network, and the associated CRUs, are present within each $\frac{1}{2}$ by 1 $\mu$m window. Note that in rat EDL and SOL muscles two T tubule networks are located on either side of the Z line, at a longitudinal distance of considerably less than 1 $\mu$m from each other and the positions of CRUs are quite faithfully duplicated in the two networks. The number of feet given in the histograms is double that found at each position along a single T network.

Several noteworthy points come out of this analysis. As may be expected, T tubules are seen at variable angles as one moves along the strip. Wherever T tubules are perpendicular to the strip more feet are present within the selection window, while few feet are included where the T tubule is mostly parallel to the strip. The distances between minima and maxima of the histogram are related to the size of the myofibrils and to the size of the CRUs (compare Figs. 3 and 4 for twitch fibers versus Fig. 5 for a tonic fiber). Over short distances, the maxima are quite regularly spaced, with a period closely corresponding to the diameter of the myofibrils. In the frog fibers the differences between maxima and minima are smaller than in the rat fibers. In the tonic fibers, maxima are separated by larger distances due both to the
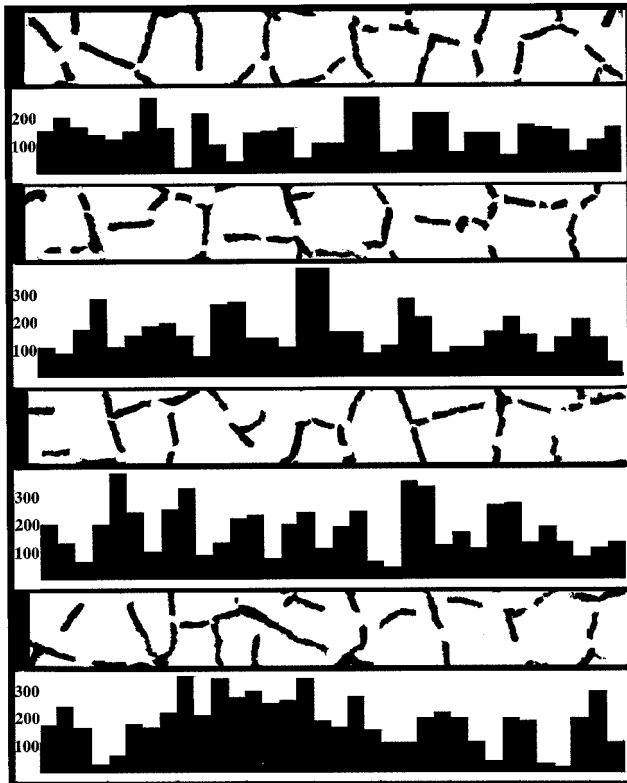
FIGURES 3–6 In each figure, 1-$\mu$m-wide strips cut from cross-section images of Golgi-infiltrated fibers alternate with histograms representing the content of feet in ½-$\mu$m-wide by 1-$\mu$m-deep windows located at ¼-$\mu$m intervals along the strip (see text for details). The images show only the junctional segments of the T network, belonging to CRUs. The wide spaces are occupied by myofibrils and some mitochondria. Two rows of feet cover the two T tubule surfaces above and below the image. Note how the content of feet in each window varies depending on the orientation of the T network relative to a viewer observing the strips from bottom to top. The views are equivalent to those seen within a confocal image obtained by scanning a fiber with a line scan that follows the direction of the Z line. In the rat fibers calculation of feet content within each window takes into account the fact that two T tubule networks are located at short intervals on either side of the Z line. Rat EDL.

larger size of the myofibrils and to the large separation between CRUs along the T tubule network. In all muscles, but less so in the frog ileofibularis, the difference in feet content between the minima and maxima are quite large (10- to 20-fold) and in addition there is a 2–3-fold variability in the size of the maxima. Interestingly, the number of feet contained in some of the selection windows of the tonic fibers are as large as those for the twitch fibers. However, such maxima are rarer in tonic fibers.

### Cardiac muscle

For cardiac muscle the analysis required serial sections, because we failed to obtain Golgi infiltration of consistent quality. Profiles of T tubule and junctional SR were marked in short series of serial sections and used to reconstruct the disposition of CRUs within portions of muscle fibers. As for
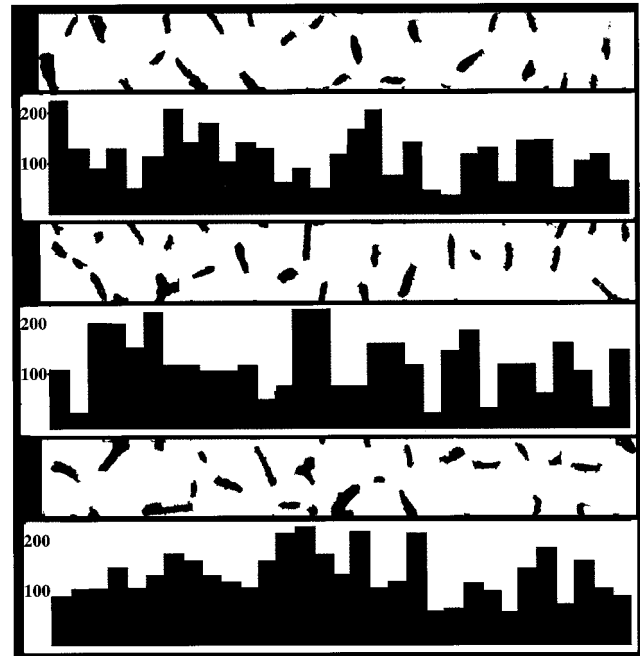


FIGURE 4 Rat soleus (See legend to Fig. 3).

skeletal muscle fibers, 1 $\mu$m wide strips were cut from the reconstructed images and nonjunctional T tubule profiles were erased. To obtain truly random views, the strips were oriented at various angles within the same region of the cell. The orientation of CRUs in cardiac muscle is different from
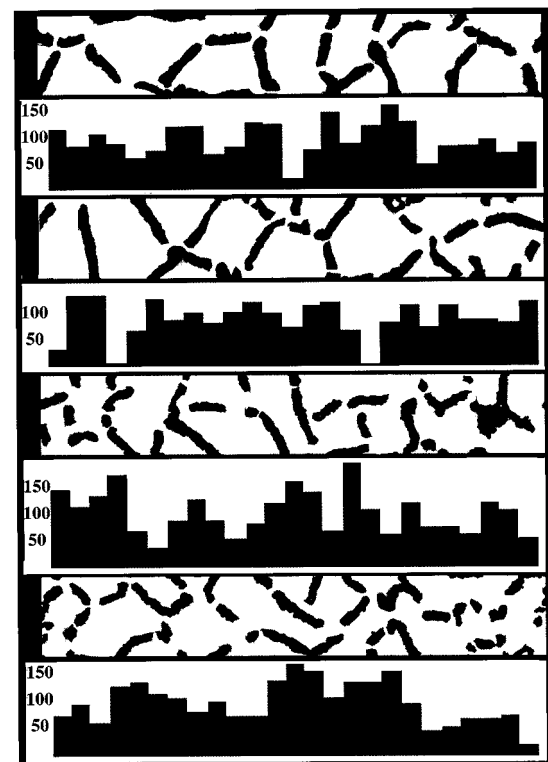


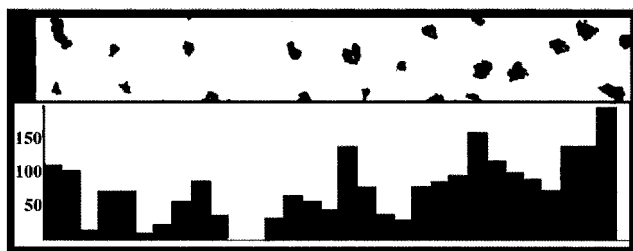FIGURE 5 Frog ileofibularis (See legend to Fig. 3).

FIGURE 6   Tonic fiber (See legend to Fig. 3).



that in skeletal muscle, since the junctional faces of SR and T tubules are mostly in planes parallel rather than perpendicular to the fiber long axis. The content of feet in each CRU portion contained within the selection window was roughly approximated by assuming that the visible length of junction is the true length of SR-T tubule contact and that junctions extend for a depth of four feet in the direction parallel to the fiber's long axis. The strips and their respective histograms are shown in Fig. 7 for mouse left ventricle and Fig. 8 for rat left ventricle.

In cardiac muscle the distances between maxima are much larger and more variable than in skeletal muscle. In addition, many selection windows show null content of feet. This is due to the presence of large mitochondria and glycogen deposits in the cytoplasm of the fiber.

## The spacing between Ca²⁺ release units

Modeling of the interaction between adjacent CRUs is critically dependent on knowing the distance between one unit and its immediate neighbor. We measured the edge-to-edge distance between each CRU and its closest neighbors in a small sample of skeletal and cardiac muscles. The results are shown in Table 3. For each CRU, the shortest distance between it and all its neighbors was measured; larger distances were ignored. The reason for measuring the nearest distances is given in the Discussion.

In skeletal muscle, the distance between CRUs depends on the length of free T tubule intercalated between the junctional T tubule segments forming triads (see Fig. 2, *A–C*). Very fast- and fast-twitch fibers have closely spaced CRUs (average minimum distance ~100 nm, or three times the distance between adjacent feet). CRUs cover most of the T tubule network. Slow tonic fibers have widely spaced CRUs (avg. minimum distance 700 nm), with a large proportion of the T tubule in the form of free segments. Slow-twitch fibers are in between.

In avian myocardium, we compared the minimum distance separating peripheral couplings to the minimum distance between EjSR elements. The former were measured in FF replicas of the surface membrane, the latter in thin sections. The minimum distance between adjacent peripheral couplings, 472 ± 5 nm (mean ± 1 SEM, $n = 3402$), is significantly larger than the average distance between EjSR elements, 135 ± 15 nm ($n = 263$). In rat and mouse
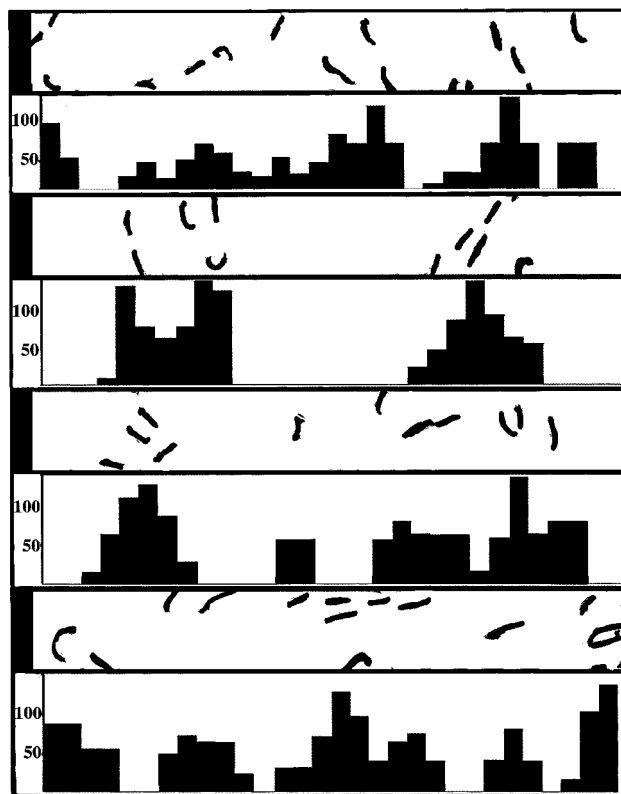
FIGURES 7 and 8   As in the previous figures, 1-$\mu$m strips have been cut from cross-sections of fibers from the left ventricle showing the position and size of T-SR junctions. The junctions were reconstructed from serial sections. Note that in this case the T and SR junctional faces are oriented perpendicular to the image plane. Feet contents were estimated by assuming that the junctions extend for a depth of four feet in the plane perpendicular to the image. This is an approximation. Feet content of adjacent windows vary as in skeletal muscle, but the distances between maxima are much larger, due to larger size of the myofibrils and to the presence of numerous mitochondria. Mouse ventricle.

myocardium the minimum distance between CRUs along T tubules is comparable to the distance between peripheral couplings on the chicken external surface (300–400 nm).

## DISCUSSION

Spontaneous and induced calcium release are due to the summed action of discrete ryanodine receptors. The nature of small calcium release events detected using calcium indicators and called calcium sparks is greatly debated. Sparks may be due to the activity of a single channel, the opening of few neighboring channels that are perhaps functionally linked, or to the ensemble opening of several channels (Cheng et al., 1993, 1995; Lipp and Niggli, 1994, 1996; Tsugorka et al., 1995; Klein et al., 1996; Parker et al., 1996; Marx et al., 1998). The location of spontaneous and induced calcium release events coincides with the known location of T tubules (Cheng et al., 1993, 1996; Escobar et al., 1994; Klein et al., 1996; Parker et al., 1996; Cleeman et al., 1998; Hollingworth et al., 1998). This is consistent with the struc-

tural location of RyRs at T tubules associated CRUs. The apparent early increase of calcium at the level of the M line in frog fibers (Escobar et al., 1994) has not been confirmed (Hollingworth et al., 1998) and also it could not be explained on the basis of the data by Dulhunty et al. (1992) in which possible extrajunctional RyRs were detected in close proximity to the junctional ones.

The data in this manuscript offer three different levels of information on the clustering of ryanodine receptors within CRUs that are relevant to spatial modeling of calcium release. First we give the feet content and the feet disposition in individual CRUs. Both are needed for modeling at the single spark level, and they should be useful in debating whether simultaneous activity of all channels in a CRUs may be responsible for a spark. The data are collected from a relatively small sample for each muscle, and the reader is referred to the Methods section for a cautionary note. As an indication of data reliability, twofold differences in average feet content (e.g., rat fast-twitch versus rat slow-twitch; chicken cardiac versus dog cardiac) are quite well visible to the eye (see Fig. 1) and thus they certainly are significant. Note that in all but one skeletal muscle the range of feet content was obtained for individual couplons and the results show a variation of up to 10-fold for a given muscle. This is not due to the inclusion of widely different types of fibers in the counts (see Methods) but to the fact that individual triads, even when side-by-side, can vary considerably in their feet content (see further comments below). If sparks were due to the activation of all RyRs within a couplon, their amplitude would be expected to vary by a factor of up to 10 within an individual muscle fiber. A second important consideration is that couplons contain a large number of feet, particularly in cardiac muscle. If all RyRs in a given couplon were activated simultaneously, 100 or more feet would be releasing during a single event.

In skeletal muscle the average size of couplons is related to fiber type properties in some but not all instances: faster fibers have larger couplons. This observation is subject to at least two different interpretations. It is tempting to speculate that larger couplons would be an advantage if calcium release was internally boosted within each couplon and if this amplification involved the entire couplon or most of it. However, the table shows two important exceptions to the general trend: superfast muscles in male and female toadfish have CRUs of very different size, and the size of CRUs in slow tonic fibers is as large as that in fast fibers, despite at least a 10-fold difference in rate of contraction. The relatively large content of feet in the latter type of fibers is hard to fit into an amplification scheme, although tonic fibers have similarities in activation kinetics and independence from extracellular calcium with twitch fiber (Gilly and Hui, 1980).

An alternate and more likely reason for larger CRUs and couplons is simply that they tend to cover larger portions of the T tubules, thus increasing the density of feet in the fiber volume and the rate of calcium release, without need of an amplification. Fast-twitch fiber types in mammalian muscle

have shorter nonjunctional T tubule segments together with longer junctional segments, resulting in a higher feet density than slow-twitch fibers (Franzini-Armstrong et al., 1988; Appelt et al., 1989). The same trend holds in cardiac muscle, where muscles from smaller animals have faster beating hearts and very frequent CRUs (Forbes, 1990; Forbes et al., 1984, 1985). The finch myocardium is the most extreme example, with an almost continuous net of very closely spaced CRUs at every Z line level (Sommer et al., 1997).

The second level of analysis is illustrated in Figs. 3–8. Note that each figure presents the case for a single fiber and that some variations are to be expected in other fibers from the same muscle. The aim of the figures is to provide an indication of the number of feet and of couplons that are detected in a line scan along the level of a single T tubule. Initiation of a calcium release event within a couplon is due to the stochastic activation of a single RyR channels for both spontaneous and evoked sparks (Lopez-Lopez et al., 1994; Cannell et al., 1995). Thus the probability of detecting a spark at any given site should be dependent on the number of feet that are located within the thickness of the detection strip at that site. The analysis indicates that the feet content in contiguous small volumes at the level of a Z line varies at intervals that roughly correspond to the diameter of the myofibrils or, in the case of cardiac muscle, to the size of the space occupied by contiguous myofibrils and mitochondria. In addition, occasional sites have considerably higher content of feet within the small volume considered than most other sites. In cardiac muscle calcium release sites have been detected at intervals along the Z lines that are related to the spacings between peaks of feet density shown
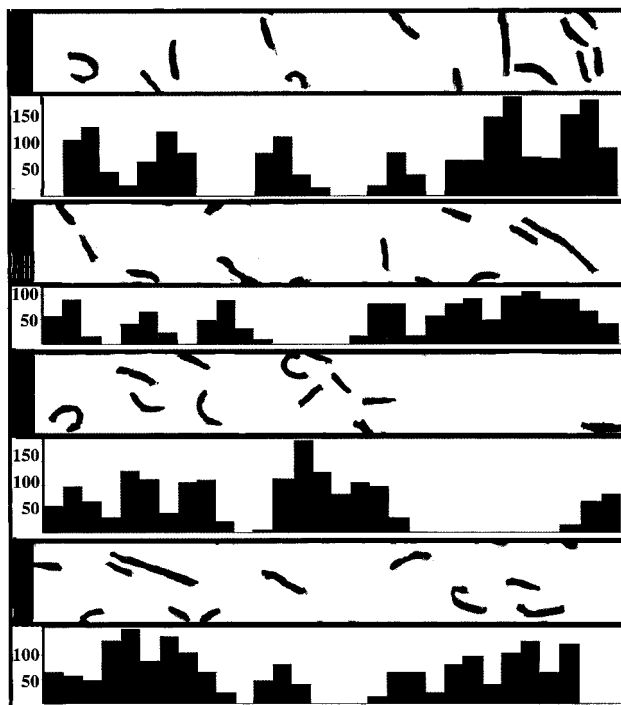


FIGURE 8 Rat ventricle (See legend to Fig. 7).

in this work (Parker et al., 1996; Cleeman et al., 1998). Variations in feet densities along the line scan do not account for the burst type behavior of sparking activity at a given site (Parker and Wier, 1997).

Figs. 3–8 indicate that more than one CRU (or part thereof) may be contained within a given site within the detection strip. This may account for the observation that sparks, at least in cardiac muscle, have occasionally been resolved into multiple (two to three) closely spaced peaks (Parker et al., 1996; Blatter et al., 1997). This behavior might indicate interaction between adjacent CRUs but, due to limited resolution of light optics, it is unlikely to represent the activity of two independent channels within the same CRU.

The data in the figures are based on a $z$ axis spread of 1 $\mu$m. In order to account for lower $z$ axis resolution and the detection of sparks even when the calcium release site of origin is close to but outside the focus window (Pratusevich and Balke, 1996), it is simply necessary to broaden the strips shown in Figs. 3–6.

Data in the third set give the minimum distance separating the edges of adjacent CRUs either within a T tubule network or over the fiber surface. Variations in the distance between CRUs are important in modulating the effect that calcium released by one unit may have on the adjacent ones. Recent evidence for undetectable and/or very small calcium release events (quarks) and for propagated calcium waves would suggest a hierarchical progression (Lipp and Niggli, 1997) from quark, involving a single channel, to spark, involving several channels in a CRU, to propagated calcium wave, involving several CRUs (Tsugorka et al., 1995; Lipp and Niggli, 1996–1998; Cheng et al., 1996; Parker et al., 1996; Wier et al., 1997; Shirokova and Rios, 1997; Shirokova et al., 1998). Thus the activity of one CRU may affect that of its neighbor leading to spread of activation across the fiber. In the case of cardiac fibers that have no T tubules, this indirect activation of centrally located CRUs (the EjSR) must be the norm (Sommer et al., 1991, 1997; Dolber and Sommer, 1994). In cardiac muscle we find that CRUs associated with surface membrane and T tubules, which have the potential of being activated independently of each other, are more distantly spaced than CRUs not associated with either surface membrane or T tubules, which require spread of activation from neighboring CRUs.

In skeletal muscle membrane potential-independent spread of activity does not occur, since the effect of exterior membrane depolarization on SR calcium release is strictly local (Huxley and Taylor, 1958) and the physiological steep relationship between T tubule voltage and calcium release holds under cytoplasmic buffering and threshold activation conditions that would not allow effects of calcium released by one CRU to reach others (Pape et al., 1995). Thus sparks of variable sizes in frog skeletal muscle (Klein et al., 1996) are more likely to be due to variable number of activated feet within a single couplon than to spread of activation from one CRU to another. Comparing inter-CRU distances between skeletal and cardiac muscles, we find that in some skeletal muscle CRUs are as closely spaced as EjSR is in the avian cardiac muscle. The overall inhibitory effect of calcium on SR calcium release in skeletal muscle (Jong et al., 1995; Pape et al., 1998) may contribute to the fact that closely spaced CRUs do not affect each other in skeletal muscle.

## REFERENCES

Anderson, P. A., A. Manring A., J. R. Sommer, and E. A. Johnson. 1976. Cardiac muscle: an attempt to relate structure to function. *J. Mol. Cell. Cardiol.* 8:123–143.

Appelt, D., B. Buenvaje, C. Champ, and C. Franzini-Armstrong. 1989. Quantitation of feet containing two types of muscle fibers from hind limb of the rat. *Tissue and Cell.* 21:783–794.

Appelt, D., V. Shen, and C. Franzini-Armstrong. 1991. Quantitation of Ca ATPase, feet and mitochondria in super fast muscle fibres from the toadfish, Opsanus tau. *J. Muscle Res. Cell Motil.* 12:543–552.

Blatter, L. A., J. Huser, and E. Rios. 1997. Sarcoplasmic reticulum Ca2+ release flux underlying Ca2+ sparks in cardiac muscle. *Proc. Natl. Acad. Sci. USA.* 94:4176–4181.

Block, B. A., A. Leung, K. P. Campbell, and C. Franzini-Armstrong. 1988. Structural evidence for direct interaction between the molecular components of the transverse tubules/sarcoplasmic reticulum junction in skeletal muscle. *J. Cell Biol.* 107:2587–2600.

Cannell, M. B., H. Cheng, and W. J. Lederer. 1995. The control of calcium release in heart muscle. *Science.* 268:1045–1049.

Carl, S. L., K. Felix, A. H. Caswell, N. R. Brandt, J. P. Brunschwig, G. Meissner, and D. G. Ferguson. 1995. Immunolocalization of sarcolemmal dihydropyridine receptor and sarcoplasmic reticular triadin and ryanodine receptor in rabbit ventricle and atrium. *J. Cell Biol.* 129:672–682.

Cheng, H., M. B. Cannell, and W. J. Lederer. 1995. [Ca$^{2+}$]i during excitation-contraction coupling in cardiac myocytes. *Circ. Res.* 76:236–241.

Cheng, H., W. J. Lederer, and M. B. Cannell. 1993. Calcium sparks: elementary events underlying excitation-contraction coupling in heart muscle. *Science.* 262:740–744.

Cheng, H., M. R. Lederer, W. J. Lederer, and M. B. Cannell. 1996. Calcium sparks and [Ca$^{2+}$]$_i$ waves in cardiac myocytes. *Am. J. Physiol.* 270:C148–C159.

Cleeman, L., W. Wang, and M. Morad. 1998. Two-dimensional confocal images of organization, density, and gating of focal Ca2+ release sites in rat cardiac myocytes. *Proc. Natl. Acad. Sci. USA.* 95:10984–10989.

Costantin, L. L., R. J. Podolsky, and L. W. Tice. 1967. Calcium and activation of frog slow fibres. *J. Physiol.* 188:261–271.

Cullen, M. J., S. Hollingworth, and M. W. Marshall. 1984. A comparative study of the transverse tubular system of the rat extensor digitorum longus and soleus muscles. *J. Anat.* 138:297–308.

Dolber, P. C., and J. R. Sommer. 1994. Corbular sarcoplasmic reticulum of rabbit cardiac muscle. *J. Ultrastruct. Res.* 87:190–196.

Dulhunty, A. F. 1984. Heterogeneity of T-tubule geometry in vertebrate skeletal muscle fibres. *J. Muscle Res. Cell Motil.* 5:333–474.

Dulhunty, A. F. 1989. Feet, bridges, and pillars in triad junctions of mammalian skeletal muscle: their possible relationship to calcium buffers in terminal cisternae and T-tubules and to excitation-contraction coupling. *J. Membr. Biol.* 109:73–83.

Dulhunty, A. F., P. R. Junankar, and C. Stanhope. 1992. Extra-junctional ryanodine receptors in the terminal cisternae of mammalian skeletal muscle fibres. *Proc. R. Soc. Lond. B.* 247:69–75.

Escobar, A. L., J. R. Monck, J. M. Fernandez, and J. L. Vergara. 1994. Localization of the site of Ca2+ release at the level of a single sarcomere in skeletal muscle fibres. *Nature.* 367:739–741.

Forbes, M. S. 1990. Ultrastructure of the myocardium of the least shrew, *Cryoptis parva*. *Anat Rec*. 226:57–70.

Forbes, M. S., L. A. Hawkey, S. K. Jjirge, and N. Sperelakis. 1985. The sarcoplasmic reticulum of mouse heart: its divisions, configurations and distribution. *J. Ultrastruct. Res*. 93:1–16.

Forbes, M. S., L. A. Hawkey, and N. Sperelakis. 1984. The transverse-axial tubular system (TATS) of mouse myocardium: its morphology in the developing and adult animal. *Am. J. Anat*. 170:143–162.

Forbes, M. S., and N. Sperelakis. 1980. Membrane systems in skeletal muscle of the lizard *Anolis carolinensis*. *J. Ultrastruct. Res*. 73:245–261.

Forbes, M. S., and E. E. van Niel. 1988. Membrane systems of guinea pig myocardium. Ultrastructure and morphometric studies. *Anat. Rec*. 222: 362–379.

Franzini-Armstrong, C. 1973. Studies of the triad. IV. Structure of the junction in frog slow fibers. *J. Cell Biol*. 56:120–128.

Franzini-Armstrong, C. 1996. Ultrastructural studies on feet/ryanodine receptors. *In* Ryanodine Receptors. V. Sorrentino, editor. CRC Press, New York. 1–16.

Franzini-Armstrong, C., C. Champ, and D. G. Ferguson. 1988. Discrimination between fast and slow-twitch fibres of guinea pig skeletal muscle using the relative surface density of junctional transverse tubule membrane. *J. Muscle Res. Cell Motil*. 9:403–414.

Franzini-Armstrong, C., W. F. Gilly, E. Aladjem, and D. Appelt. 1987. Golgi stain identifies three types of fibers in fish muscle. *J. Muscle Res. Cell Motil*. 8:418–427.

Franzini-Armstrong, C., and A. O. Jorgensen. 1994. Structure and development of e-c coupling units in skeletal muscle. *Annu. Rev. Physiol*. 56:509–534.

Franzini-Armstrong, C., and L. D. Peachey. 1982. A modified Golgi black reaction method for light and electron microscopy. *J. Histochem. Cytochem*. 30:99–105.

Gilly, W. F., and E. Aladjem. 1987. Physiological properties of three muscle fibre types controlling dorsal fin movements in a flatfish, *Citharichthys sordidus*. *J. Muscle Res. Cell Motil*. 8:407–417.

Gilly, W. F., and C-S. Hui. 1980. Mechanical activation in slow and twitch skeletal muscle fibres of frog. *J. Physiol. (Lond)*. 30:137–156.

Hollingworth, S., C. Soeller, S. M. Baylor, and M. B. Cannell. 1998. Local calcium gradients during activation of frog skeletal muscle measured with MG-Green and Fluo-3. *Biophys. J*. 74:235a. (Abstr.).

Huxley, A. F., and R. E. Taylor. 1958. Local activation of skeletal muscle fibers. *J. Physiol. (Lond)*. 144:426–441.

Jewett, P. H., S. D. Leonard, and J. R. Sommer. 1973. Chicken cardiac muscle: its elusive extended junctional sarcoplasmic reticulum and sarcoplasmic reticulum fenestrations. *J. Cell Biol*. 56:595–600.

Jong, D. S., P. C. Pape, S. M. Baylor, and K. W. Chandler. 1995. Calcium inactivation of calcium release in frog cut muscle fibers that contain millimolar EGTA or Fura-2. *J. Gen. Physiol*. 106:337–388.

Junker, J., J. R. Sommer, and G. Meissner. 1994. Extended junctional sarcoplasmic reticulum of avian cardiac muscle contains functional ryanodine receptors. *J. Biol. Chem*. 269:1627–1634.

Klein, M. G., H. Cheng, L. F. Santana, Y. H. Jiang, Y. H. Lederer, and M. F. Schneider. 1996. Two mechanisms of quantized calcium release in skeletal muscle. *Nature*. 379:455–458.

Lipp, P., and E. Niggli. 1994. Modulation of Ca$^{2+}$ release in cultured neonatal rat cardiac myocytes. Insight from subcellular release patterns revealed by confocal microscopy. *Circ. Res*. 74:979–990.

Lipp, P., and E. Niggli. 1996. Submicroscopic calcium signals as fundamental events of excitation-contraction coupling in guinea-pig cardiac myocytes. *J. Physiol. (Lond)*. 492:31–38.

Lipp, P., and E. Niggli. 1997. A hierarchical concept of cellular and subcellular Ca$^{2+}$ signaling. *Prog. Biophys. Mol. Biol*. 65:265–296.

Lipp, P., and E. Niggli. 1998. Fundamental Ca$^{2+}$ release events revealed by two-photon excitation photolysis of caged calcium in guinea pig cardiac myocytes. *J. Physiol. (Lond)*. 508:801–809.

Lopez-Lopez, J. R., P. S. Shacklock, C. W. Balke, and W. G. Wier. 1994. Local, stochastic release of Ca$^{2+}$ in voltage-clamped rat heart cells: visualization with confocal microscopy. *J. Physiol. (Lond)*. 480:21–29.

Marx, S. O., K. Ondrias, and A. R. Marks. 1998. Coupled gating between individual skeletal muscle Ca2+ release channels (ryanodine receptors). *Science*. 281:818–821.

Page, S. G. 1965. A comparison of the fine structure of frog slow and twitch fibers. *J. Cell Biol*. 26:477–497.

Page, S. G., and R. Niedergerke. 1972. Structures of physiological interest in the frog heart ventricle. *J. Cell Sci*. 11:179–203.

Pape, P. C., D. S. Jong, and K. W. Chandler. 1995. Calcium release and its voltage dependence in frog cut muscle fibers equilibrated with 20 mM EGTA. *J. Gen. Physiol*. 106:259–336.

Pape, P. C., D. S. Jong, and K. W. Chandler. 1998 Effects of partial sarcoplasmic reticulum calcium depletion on calcium release in frog cut fibers equilibrated with 20 mM EGTA. *J. Gen. Physiol*. 112:263–265.

Parker, I., and W. G. Wier. 1997. Variability in frequency and characteristics of Ca2+ sparks at different release sites in rat ventricular myocytes. *J. Physiol. (Lond)*. 505:337–344.

Parker, I., W. J. Zang, and W. G. Wier. 1996. Ca$^{2+}$ sparks involving multiple Ca$^{2+}$ release sites along the Z-lines in rat heart cells. *J. Physiol. (Lond)*. 491:663–668.

Peachey, L. D., and A. F. Huxley. 1962. Structural identification of twitch and slow striated muscle fibers in the frog. *J. Cell Biol*. 13:177–180.

Pratusevich, V. R., and C. W. Balke. 1996. Factors shaping the confocal image of the calcium spark in cardiac muscle cells. *Biophys. J*. 71: 2942–2957.

Protasi, F., X-H. Sun, and C. Franzini-Armstrong. 1996. Formation and maturation of calcium release units in developing and adult avian myocardium. *Dev. Biol*. 173:265–278.

Rios, E., and M. D. Stern. 1997. Calcium in close quarters: microdomain feedback in excitation-contraction coupling and other cell biological phenomena. *Annu. Rev. Biophys. Biomol. Struct*. 26:47–82.

Rome, L. C., D. A. Syme, S. Hollingworth, S. L. Lindstedt, and S. M. Baylor. 1996. The whistle and the rattle: the design of sound producing muscles. *Proc. Natl. Acad. Sci. USA*. 93:8095–8100.

Shirokova, N., J. Garcia, and E. Rios. 1988. Local calcium release in mammalian skeletal muscle. *J. Physiol*. 512(Pt 2):377–384.

Shirokova, N., and E. Rios. 1997. Small event Ca2+ release: a probable precursor of Ca2+ sparks in frog skeletal muscle. *J. Physiol*. 502:3–11.

Sommer, J. R. 1982. Ultrastructural considerations concerning cardiac muscle. *J. Mol. Cell. Cardiol*. 14:77–83.

Sommer, J. R. 1995. Comparative anatomy: in praise of a powerful approach to elucidate mechanisms translating cardiac excitation into purposeful contraction. *J. Mol. Cell. Cardiol*. 27:19–35.

Sommer, J. R., E. Bossen, H. Dalen, P. C. Dolber, T. High, P. Jewett, E. A. Johnson, J. Junker, S. R. Leonard, R. Nassar, and P. Ingram. 1991. To excite a heart: a bird's view. *Acta Physiol. Scand. Suppl*. 599:5–21.

Sommer, J. R., T. High, P. Ingram, R. Nassar, I. Taylor, and D. Kopf. 1998. Couplings and couplons. *J. Gen. Physiol*. 112:14a. (Abstr.).

Sommer, J. R., T. High, and I. Taylor. 1997. The geometry of the EJSR Z-rete in avian cardiac muscle. *Proc. 55Th Annual Meeting, Microscopy Soc. Am*. G. W. Bailey and A.J Garratt-Reed, editors. San Francisco Press. 20–21.

Stern, M. D., G. Pizarro, and E. Rios. 1997. Local control model of excitation-contraction coupling in skeletal muscle. *J. Gen. Physiol*. 110:415–440.

Tsugorka, A., E. Rios, and L. A. Blatter. 1995. Imaging elementary events of calcium release in skeletal muscle cells. *Science*. 269:1723–1726.

Wier, W. G., H. E. ter Keurs, E. Marban, W. D. Gao, and C. W. Balke. 1997. Ca2+ "sparks" and waves in intact ventricular muscle resolved by confocal imaging. *Circ. Res*. 81:462–469.